Design and Semisynthesis of Photoactive Myoglobin Bearing Ruthenium Tris(2,2′-bipyridine) Using Cofactor-Reconstitution

Itaru Hamachi,*,† Shigeaki Tanaka,† Shinya Tsukiji,† Seiji Shinkai,† and Shigero Oishi‡

Department of Chemistry & Biochemistry, Graduate School of Engineering, Kyushu University, Fukuoka 812-81, Japan, and Department of Chemistry, School of Science, Kitasato University, Sagamihara, Kanagawa 228, Japan

Received December 2, 1997

A new strategy for semisynthesis of a photoactivatable redox protein is described. Three protohemin molecules with ruthenium tris(2,2′-bipyridine) attached by different spacers were synthesized. The $Ru(bpy)_3$-protohemins were incorporated into the heme crevice of apomyoglobin (apo-Mb) to yield semisynthetic Mbs carrying $Ru(bpy)_3$ as a photosensitizer ($Ru(bpy)_3$-Mb). The photoactivation properties and the reaction mechanisms of $Ru(bpy)_3$-Mbs were investigated by steady-state photoirradiation and laser flash photolysis. The photoactivation of $Ru(bpy)_3$-Mbs was spectrophotometrically demonstrated by comparison with an intermolecular control, namely an equimolar mixture of $Ru(bpy)_3$ and native Mb. The spacer structure considerably influenced net activation efficiency over a wide pH range as measured by steady-state visible light irradiation and quantum yield. Laser flash photolysis yielded the rate of the photoinduced electron transfer (ET) from the lifetime of the excited $Ru(bpy)_3$ ($k_{et} = 4.4 \times 10^7\ s^{-1}$ for Mb(**1b**) and $k_{et} = 3.7 \times 10^7\ s^{-1}$ for Mb(**1c**)) and the back ET rate ($k_{back} = (2.0-3.7) \times 10^7\ s^{-1}$ for Mb(**1b**) and $k_{back} = (1.4-2.4) \times 10^7\ s^{-1}$ for Mb(**1c**)) from the decay of the transient absorption. These data consistently explained the results of the *net* photoreaction as follows. (i) The intermolecular control system was less photoactivated because little ET occurred from the excited state of $Ru(bpy)_3$ to Mb. (ii) The short lifetime of the charge-separated state after photoinduced ET greatly decreased the photoactivation efficiency of $Ru(bpy)_3$-Mb with the shortest spacer. (iii) The photochemical and photophysical data of the other two $Ru(bpy)_3$-Mb derivatives (the net photoreaction, quantum yield, and ET/back ET rates) were essentially identical, indicating that flexible spacers consisting of oxyethylene units do not rigidly fix the distance between $Ru(bpy)_3$ and the heme center of Mb. In addition, $Ru(bpy)_3$-Mbs were highly photoactivated under aerobic conditions in a manner similar to that under anaerobic conditions, although O_2 usually quenches the photoexcited state of $Ru(bpy)_3$. This was probably due to the accelerated intramolecular ET from $*Ru(bpy)_3$ to heme, not to O_2 in $Ru(bpy)_3$-Mbs. We therefore showed that visible light affects the content of O_2-bound Mb even in air.

Introduction

Electron transfer (ET) is considered to be one of the most important and fundamental reactions in a number of biological phenomena, particularly in energy conversion systems such as respiration and photosynthesis.[1] Efforts to elucidate the physical and chemical aspects of ET events include both theoretical and experimental approaches.[2] It is generally accepted that spatially (e.g., distance, orientation, and microenvironment) defined ET is essential for reactions to proceed efficiently, along with finely tuned potentials of redox partners.

In biological systems, redox active proteins and enzymes such as hemoproteins (a series of cytochromes), ferredoxins containing an iron−sulfur cluster, flavoenzymes and PQQ- or NAD(H)-dependent enzymes play key roles.[3] The redox state of these proteins and enzymes directly affects *net* chemical reactivity. This indicates that an *artificially* controlled electron injection into and/or abstraction from the redox center can regulate the *net* activity of enzymes or multienzyme systems. However, it is difficult to artificially inject into or extract electrons from the active sites since these are often buried in the hydrophobic core of the protein matrix.[4] A convenient means is required for constructing a spatially fixed ET pathway to promote electrical communication from the bulk solution to the active site of a protein.

We recently proposed an approach with which to control the redox state of proteins by photoinduced ET: covalent attachment of a photosensitizer ($Ru(bpy)_3$) to a hemoprotein (myoglobin-(Mb)) using cofactor reconstitution.[5] We photoswitched a semisynthetic Mb from a resting to an active state. That is, Mb was converted to a photoactive hemoprotein. This article discusses a detailed study of the photoreactions of three semisynthetic Mbs bearing $Ru(bpy)_3$. The kinetic mechanism and the *net* photoactivation properties of semisynthetic Mbs were examined by laser photolysis and steady-state photoirradiation under both anaerobic and aerobic conditions.

Results

Design and Synthesis of Protohemin Linked to $Ru(bpy)_3$. We functionalized protohemin, the naturally occurring prosthetic group of most hemoproteins, and incorporated it into the heme

* Corresponding author. E-mail: itarutcm@mbox.nc.kyushu-u.ac.jp.
† Kyushu University.
‡ Kitasato University.

(1) Stryer, L. *Biochemistry*, 3rd ed.; Freeman: New York, 1988; pp 398−426, 517−541.
(2) (a) Marcus, R.; Sutin, N. *Biochim, Biophys. Acta* **1985**, *811*, 265. (b) Winkler, J. R.; Gray, H. B. *Chem. Rev.* **1992**, *92*, 9. (c) McLendon, G.; Hake, R. *ibid.* **1992**, 481.
(3) Chance, B.; Devaut, D. C.; Frauenfelder, H.; Marcus, R. A.; Schrieffer, J. R.; Sutin, N. *Tunneling in biological systems*; Academic Press: London, 1979; pp 303−370.

S0020-1669(97)01507-3 CCC: $15.00
Published on Web 08/07/1998

crevice of apomyoglobin (apo-Mb). X-ray structural study of native Mb has established that both propionate ends of protohemin are exposed to the protein surface.[6] Hence, molecules were modified to contain ruthenium tris(2,2′-bipyridine) at a propionate site with appropriate spacers ($Ru(bpy)_3$-hemin) to minimize the structural perturbation of the reconstituted Mb.[7] The synthetic route is shown in Scheme 1. Protoporphyrin IX monoethylester was condensed with amino derivatives of 2,2′-bipyridine (bpy) in the presence of diethylcyanophosphate, then complexed with bis-bpy dichlororuthenium ($Ru(bpy)_2Cl_2$). Ester hydrolysis was followed by iron insertion into the resultant ruthenium tris-bpy-protoporphyrin IX, to yield target $Ru(bpy)_3$-appended hemins. We prepared three heme derivatives bearing spacers at different lengths by essentially the same procedure.

Reconstitution of $Ru(bpy)_3$-Hemin with Apomyoglobin. The three $Ru(bpy)_3$-hemins were reconstituted to apo-Mb according to a slight modification of the reported procedure.[8] Spectrophotometric titration of the modified hemin with apo-Mb showed 1/1 complex formation. The absorption spectrum of the met form (oxidized form; Fe(III) state) of semisynthetic Mb bearing $Ru(bpy)_3$ ($Ru(bpy)_3$-Mb) showed a sharp Soret band at 409 nm, a Q band at 630 nm, a sharp peak at 287 nm due to bpy, and a shoulder at 457 nm due to the MLCT band of the $Ru(bpy)_3$ unit (Figure 6a, without light).[7] This is almost identical to the spectrum generated by the simple sum of an equimolar mixture of $Ru(bpy)_3$ and native Mb, indicating a lack of interaction between $Ru(bpy)_3$ and the heme site of Mb in the ground state. The reduction of the met form of $Ru(bpy)_3$-Mbs by $Na_2S_2O_4$ and the subsequent air-oxidation gave absorption spectra corresponding to those of deoxy (reduced state; Fe(II)) and oxy (dioxygen-bound state) forms, respectively. These spectra were almost identical to those of native Mb (434 and 555 nm for the deoxy form shown in Figure 1 after photoirradiation, 417, 543, and 582 nm for the oxy form shown in Figure 6a). The absorption spectra of $Ru(bpy)_3$-Mbs, the axial (sixth) ligand of which was replaced with fluoride, cyanide or azide, were essentially identical to those of the corresponding forms of native Mb. Electron paramagnetic resonance (EPR) of a frozen solution containing met-$Ru(bpy)_3$-Mbs displayed a typical high-spin state of iron(III) species ($g = 5.9$ and 2.0). Their circular dichroism (CD) and native spectra were also similar (CD peaks at 195 nm (positive) and at 208 and 222 nm (negative)).[9] The redox potential ($E_{1/2}$) of the iron site (Fe(II)/Fe(III)) was determined by thin layer spectroelectrochemistry. The $E_{1/2}$ values were 70 ± 2 for Mb(**1a**), 71 ± 10 for Mb(**1b**), and 80 ± 6 mV for Mb(**1c**) vs NHE, which are slightly more positive than that of native Mb (50 ± 10 mV).[10] All these data indicate that the $Ru(bpy)_3$-hemins were successfully reconstituted with apo-Mb (See Scheme 2).

Scheme 1

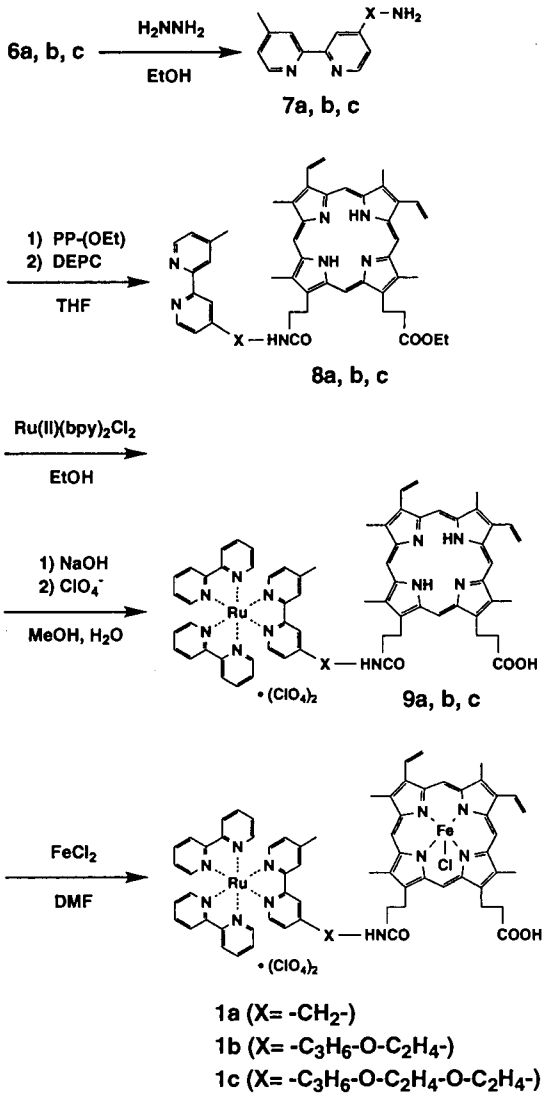

(4) Recent examples: (a) de Lumley-Woodyear, T.; Campbell, C. N.; Heller, A. *J. Am. Chem. Soc.* **1996**, *118*, 5504. (b) Kenausis, G.; Taylor, C.; Katakis, I.; Heller, A. *J. Chem. Soc., Faraday Trans.* **1996**, *92*, 4131. (c) Csoregi, E.; Laurell, T.; Katakis, I.; Heller, A.; Gorton, L. *Mikrochim. Acta* **1995**, *121*, 31. (d) Heller, A. *Acc. Chem. Res.* **1990**, *23*, 128. (e) Heller, A. *Acc. Chem. Res.* **1995**, *28*, 503. (f) Low, D. W.; Yang, G.; Winkler, J. R.; Gray, H. B. *J. Am. Chem. Soc.* **1997**, *119*, 4094. (g) Jacobs, B. A.; Mauk, M. R.; Funk, W. D.; MacGillivray, R. T. A.; Mauk, A. G.; Gray, H. B. *J. Am. Chem. Soc.* **1991**, *113*, 4390. (h) Mines, G. A.; Bjerrum, M. J.; Hill, M. G.; Casimiro, D. R.; Chang, I.; Winkler. J. R.; Gray, H. B. *J. Am. Chem. Soc.* **1996**, *118*, 1961. (i) Peterson-Kennedy, S. E.; McGourty, J. L.; Hoffman, B. M. *J. Am. Chem. Soc.* **1984**, *106*, 5010. (j) Zhou, J. S.; Tran, S. T.; McLendon, G.; Hoffman, B. M. *J. Am. Chem. Soc.* **1997**, *119*, 269. (k) McLendon, G. L.; Winkler, J. R.; Nocera, D. G.; Mauk, M. R.; Mauk, A. R.; Gray, H. B. *J. Am. Chem. Soc.* **1985**, *107*, 739. (l) McLendon, G.; Miller, J. R. *J. Am. Chem. Soc.* **1985**, *107*, 7811. (m) Scott, J. R.; McLean, M.; Sliger, S. G.; Durham, B.; Millett, F. *J. Am. Chem. Soc.* **1994**, *116*, 7356. (n) Nocek, J. M.; Sishta, B. P.; Cameron, J. C.; Mauk, A. G.; Hoffman, B. M. *J. Am. Chem. Soc.* **1997**, *119*, 2146. (o) Wuttke, D. S.; Gray, H. B.; Fisher, S. L.; Imperiali, B. *J. Am. Chem. Soc.* **1993**, *115*, 8455. (p) Casimiro, D. R.; Wong, L.; Colón, J. L.; Zewert, T. E.; Richards, J. H.; Chang, I.; Winkler, J. R.; Gray, H. B. *J. Am. Chem. Soc.* **1993**, *115*, 1485. (q) Meier, M.; Eldic, R.; Chang, I.; Mines, G. A.; Wuttke, D. S.; Winkler, J. R.; Gray, H. B. *J. Am. Chem. Soc.* **1994**, *116*, 1577. (r) Fenwick, C.; Marmor, S.; Govindaraju, K.; English, A. M.; Wishart, J. F.; Sun, J. *J. Am. Chem. Soc.* **1994**, *116*, 3169. (s) Scott, J. R.; Willie, A.; McLean, M.; Stayton, P. S.; Sliger, S. G.; Durham, B.; Millett, F. *J. Am. Chem. Soc.* **1993**, *115*, 6820. (t) Pan, L. P.; Hibdon, S.; Liu, R.; Durham, B.; Millett, F. *Biochemistry* **1993**, *32*, 8492. (u) Wang, K.; Mei, H.; Geren, L.; Miller, M. A.; Saunders: A.; Wang, X.; Waldner, J. L.; Pielak, G. J.; Durham, B.; Millett, F. *Biochemistry* **1996**, *35*, 15107. (v) Zahavy, E.; Willner, I. *ibid.* **1995**, *117*, 10581. (w) Willner, I.; Zahavy, E. *Angew. Chem., Int. Ed. Engl.* **1994**, *33*, 581. (x) Zahavy, E.; Willner, I. *J. Am. Chem. Soc.* **1996**, *118*, 12499.

(5) (a) Hamachi, I.; Tanaka, S.; Shinkai, S. *Chem. Lett.* **1993**, 1417. (b) Hamachi, I.; Tanaka, S.; Shinkai, S. *J. Am. Chem. Soc.* **1993**, *115*, 10458. (c) Hamachi, I.; Tsukiji, S.; Tanaka, S.; Shinkai, S. *Chem. Lett.* **1996**, 751. (d) Hamachi, I.; Nomoto, K.; Tanaka, S.; Shinkai, S. *Chem. Lett.* **1994**, 1139. (e) Hamachi, I.; Matsugi, T.; Tanaka, S.; Shinkai, S. *Bull. Chem. Soc. Jpn.* **1996**, *69*, 1657.

(6) Evans, S. V.; Brayer, G. D. *J. Mol. Biol.* **1990**, *213*, 885.

(7) Since $Ru(bpy)_3$ was considerably bulky, it was attached to a propionate end so as to be exposed to the solvent, not be buried in the protein matrix. Tamura, M.; Asakura, T.; Yonetani, T. *Biochim. Biophys. Acta* **1973**, *295*, 467.

(8) (a) Teals, F. W. J. *Biochim. Biophys. Acta* **1959**, *35*, 543. (b) Yonetani, T. *J. Biol. Chem.* **1967**, *242*, 5008.

(9) (a) Yonetani, T.; Schleyer, H. *J. Biol. Chem.* **1967**, *242*, 3926. (b) Puett, D. *J. Biol. Chem.* **1973**, *248*, 4623.

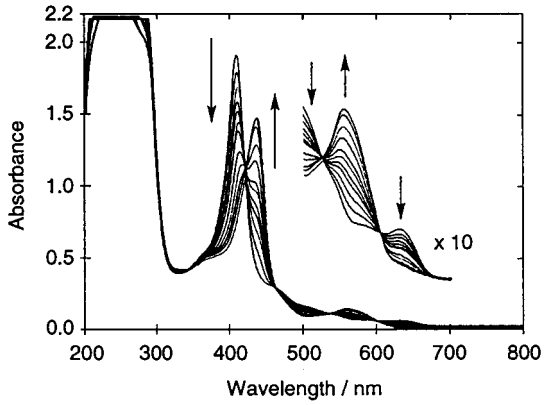

Figure 1. Absorption spectral changes of $Ru(bpy)_3$-Mb (**1b**) upon steady-state photoirradiation (wavelength cutoff below 450 nm, high-pressure Hg lamp) under anaerobic conditions: 18.6 μM $Ru(bpy)_3$-Mb (**1b**) and 10 mM Na_2EDTA in phosphate buffer (50 mM, pH 6.5) at 25 °C.

Scheme 2

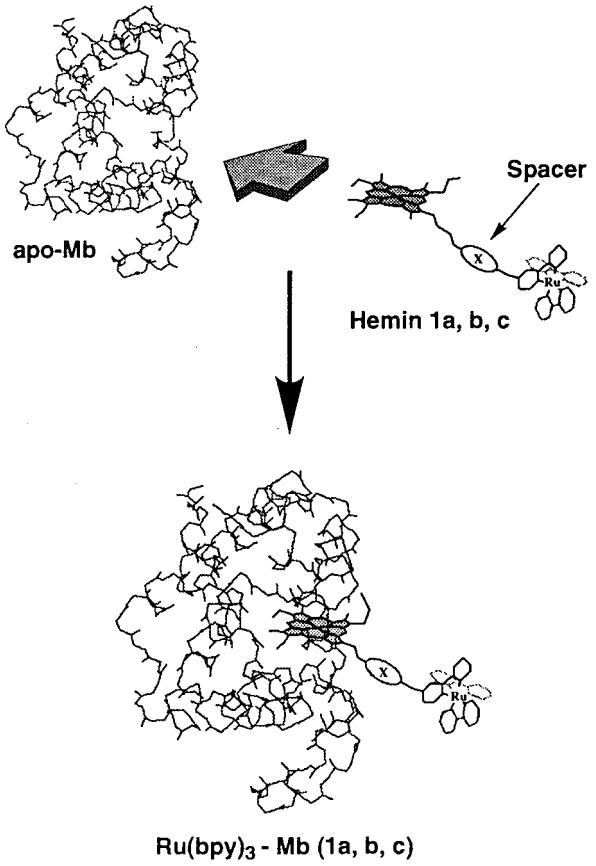

Visible Light Induced Reduction of $Ru(bpy)_3$-Mbs under Anaerobic Conditions. Since photoexcited $Ru(bpy)_3$ (*$Ru(bpy)_3$) is a powerful reductant (redox potential of -0.80 V vs NHE), the photoinduced ET from *$Ru(bpy)_3$ to iron(III) heme of met-Mb should be a downhill reaction having a high driving force (0.87−0.88 V).[11] When a solution of $Ru(bpy)_3$-Mbs was irradiated with visible light (cut off wavelength below 450 nm) in the presence of EDTA (ethylenediamine tetraacetic acid, a sacrificial donor) under Ar, the absorption maxima of Soret and Q bands due to met-Mb apparently shifted to those due to deoxy-Mb with six isosbestic points (353, 419, 462, 523, 607, and 662 nm) as shown in Figure 1. The resulting species was rapidly converted to oxy-Mb upon exposure to air, confirming that deoxy-Mb was photoproduced. This reaction did not proceed in the dark and steady state photoirradiation without EDTA did not yield deoxy-Mb. Irradiation with visible light did not spectrally change $Ru(bpy)_3$-hemins (without an apo-Mb skeleton).[12]

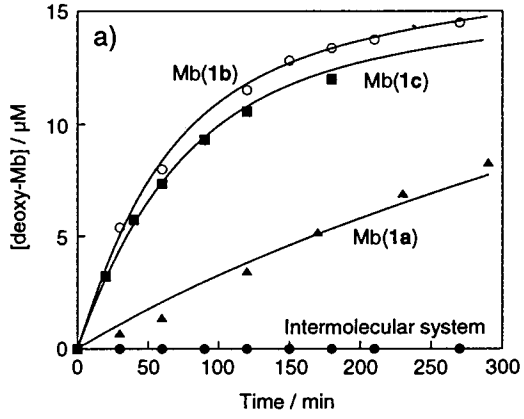

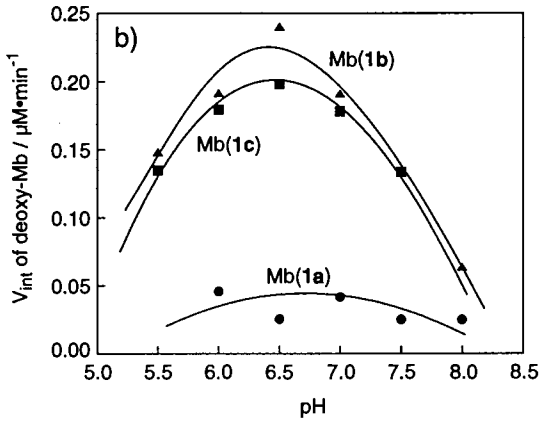

Figure 2. (a) Time courses of photogeneration of deoxy-Mb for the intramolecular (▲, $Ru(bpy)_3$-Mb (**1a**); ○, (**1b**); ■, (**1c**); $Ru(bpy)_3$-Mb (**1a**, **1b**, **1c**), 15.5 μM) and the intermolecular reaction system (a simple mixture of $Ru(bpy)_3$ and native Mb, ●, 15.5 μM) in 50 mM phosphate buffer, 10 mM Na_2EDTA, pH 6.0, 25 °C. 100 mM Na_2EDTA was used only in the case of $Ru(bpy)_3$-Mb(**1a**) because of its low efficiency. (b) Dependence of initial rate V_{int} on pH under anaerobic conditions. ●, $Ru(bpy)_3$-Mb (**1a**); ▲, (**1b**); ■, (**1c**); $Ru(bpy)_3$-Mb (**1a**, **1b**, **1c**): 18.6 μM, 50 mM phosphate buffer, 10 mM Na_2EDTA, 25 °C.

Figure 2a compares time courses of the net photoreduction of $Ru(bpy)_3$-Mbs to that of an intermolecular control system (an equimolar mixture of $Ru(bpy)_3$ and native met-Mb). No reaction proceeded in the control system, whereas Mb(**1b**) was smoothly photoreduced to completion within about 200 min.[13] The intramolecular system promoted photoinduced ET, whereas the intermolecular system did not. Mb(**1c**) was almost as efficiently photoreduced as Mb(**1b**). The reaction of Mb(**1a**), on the other hand, was 10-fold less efficient than the other two $Ru(bpy)_3$-Mbs. These results show that the spacer structure has marked effects on the photoreduction efficiency.

(10) (a) Lloyd, E.; Hildebrand, D. P.; Tu, K. M.; Mauk, A. G. *J. Am. Chem. Soc.* **1995**, *117*, 6434. (b) Brunori, M.; Saggese, U.; Rotilio, G. C.; Antonini, E.; Wyman, J. *Biochemistry* **1971**, *10*, 1604. (c) Hamachi, I.; Matsugi, T.; Wakigawa, K.; Shinkai, S. *Inorg. Chem.* **1998**, *37*, 1592.

(11) Kalyanasundaram, K. *Coord. Chem. Rev.* **1982**, *46*, 159.

(12) Hemin **1a**, **b**, and **c** dissolved in H_2O were photoirradiated in the presence EDTA.

(13) We conducted these experiments in the concentration range of 1−15 μM Mbs.

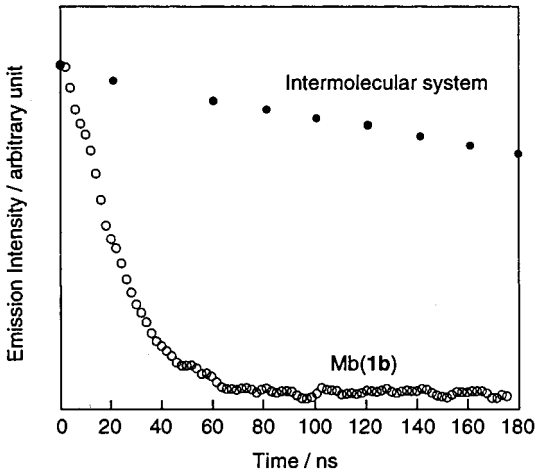

Figure 3. Emission decay of the excited state of $Ru(bpy)_3$ monitored at 610 nm for the intramolecular ($Ru(bpy)_3$-Mb) (○) and the intermolecular reaction (●), 355 nm laser excitation. $Ru(bpy)_3$-Mb (**1b**): 41.5 μM, 50 mM phosphate buffer, pH 6.0 at 27 °C.

The initial rate vs pH is plotted in Figure 2b. The spacer effect was evident over a wide pH range (pH 5.5−8.0). The photoreactions of Mb(**1b**) and Mb(**1c**) were highly efficient, whereas that of Mb(**1a**) was very slow. The profiles of the initial rate of Mb(**1b**) and Mb(**1c**) were bell-shaped, against pH bearing a maximum value at pH 6.5. The rate gradually decreased below pH 6 and slowed above pH 7.5. In the case of Mb(**1a**), the photoreduction did not completely proceed and the initial rate was very low, relative to the other two Mb derivatives. Clear bell-shaped profile of Mb(**1a**) was not observed.

Laser Flash Photolysis. We examined the mechanism of the photoreduction of $Ru(bpy)_3$-Mbs by laser flash photolysis. ET rates from the $*Ru(bpy)_3$ to iron(III) of Mb ($*Ru^{2+} \rightarrow Fe^{3+}$) were determined by measuring the emission lifetimes of the excited state of $Ru(bpy)_3$ species (Figure 3). The decay curves were analyzed by a single exponential. $*Ru^{2+} \rightarrow Fe^{3+}$ ET rate constants (k_{et}) for Mb(**1b**) and Mb(**1c**) are 4.4×10^7 and 3.7×10^7 s^{-1}, respectively. The emission decay for Mb(**1a**) could not be isolated from the excitation pulse duration (fwhm = 5 ns), indicating that k_{et} for Mb(**1a**) was greater than 2×10^8 s^{-1}. Photoinduced intermolecular electron transfer was less efficient under condition comparable to those of intramolecular $Ru(bpy)_3$-Mbs.[14]

The transient absorption spectrum of $Ru(bpy)_3$-Mb(**1b**) obtained 33 ns after laser irradiation closely agreed with the difference spectrum of the deoxy/met forms (Figure 4). The spectral baseline changed at a very early stage (within 30 ns after laser pulse). Flash photolysis of native met-Mb showed bleaching and recovery of the Soret and Q band regions within 30 ns, similar to the early stage of $Ru(bpy)_3$-Mb, suggesting that the Fe^{3+} heme portion of Mb was photoexcited and decayed within a lifetime of less than 10 ns (the estimated decay rate is over 1.2×10^8 s^{-1}). Figure 5 shows time courses of the absorbances at 560 and 630 nm due to decay of the generated deoxy form and recovery of the bleached met form, respectively. These biphasic spectral changes can be attributed to the direct photoexcitation of Fe^{3+} heme and back ET. A second kinetic phase (30 ns after the recovery of the bleached Fe^{3+}) corresponded to the process of back ET from Fe^{2+} heme to $Ru^{3+}(bpy)_3$ ($Fe^{2+} \rightarrow Ru^{3+}$; $k_{back} = (2.0-3.7) \times 10^7$ s^{-1} for Mb(**1b**), $(1.4-2.4) \times 10^7$ s^{-1} for Mb(**1c**)).[15] We did not detect the transient absorption of Mb(**1a**), probably due to the short lifetime of the charge-separated state. At high pH (pH 10), the emission

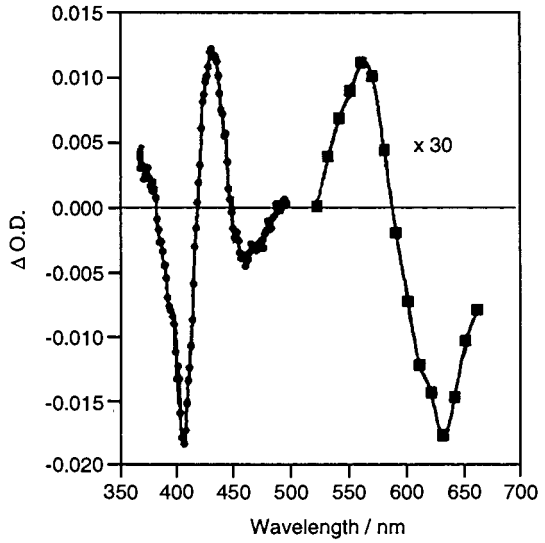

Figure 4. Transient absorption spectra of $Ru(bpy)_3$-Mb (**1b**) after laser (355 nm) irradiation (45 ns). Soret band region (355−500 nm, 41.5 μM, ●) and Q band region (525−650 nm, 100.0 μM, ■).

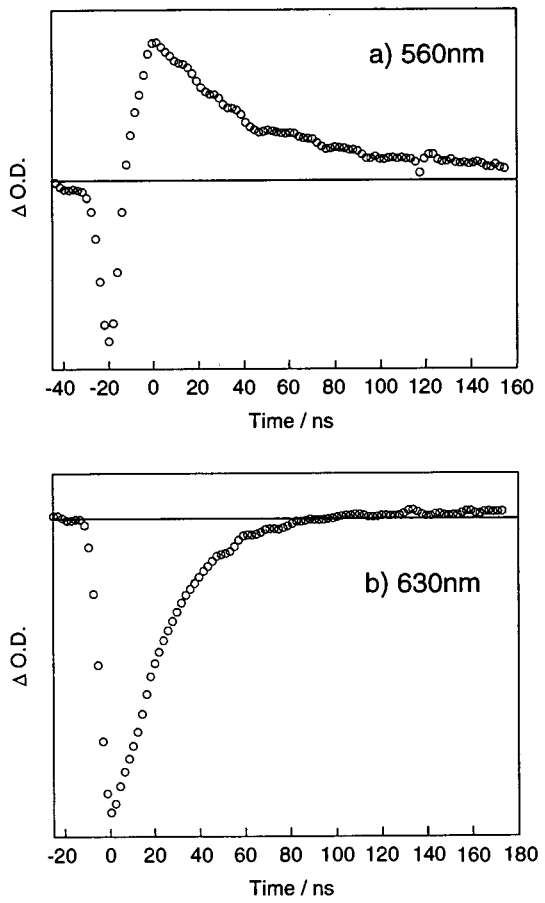

Figure 5. Typical kinetic traces at 560 nm (a) and 630 nm (b) for the $Ru(bpy)_3$-Mb (Fe^{2+}) **1b**; $Ru(bpy)_3$-Mb (**1b**); 99.6 μM, 50 mM phosphate buffer, pH 6.0, at 27 °C.

(14) The emission lifetime of $*Ru(bpy)_3^{2+}$ slightly lessened by additional native met-Mb (692 ns without native met-Mb, 607 ns with native Mb, $[Ru(bpy)_3] = [\text{native Mb}] = 41.5\ \mu M$). This quenching, however, cannot be ascribed to ET from $*Ru(bpy)_3^{2+}$ to heme-Fe^{3+} because deoxy-Mb was not detected from the transient absorption spectrum.

(15) The rate constants of the back ET calculated from the absorbance changes at 560 and 630 nm were essentially identical within the experimental errors.

Scheme 3

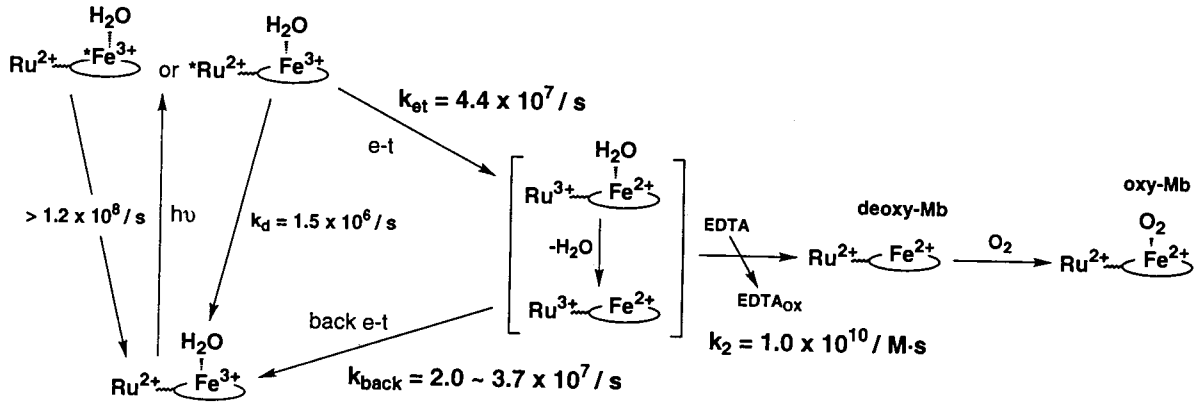

Table 1. Electron Transfer Rate Constants between Ruthenium Complex and Heme-Iron of Ru(bpy)$_3$-Mb (**1a**, **1b**, **1c**) at 20 °C, pH 6.0, 50 mM KH_2PO_4 Buffer

	Mb(**1a**)	Mb(**1b**)	Mb(**1c**)
k_{et} ($\times 10^7$ s^{-1})	*a*	4.4	3.7
k_{back} ($\times 10^7$ s^{-1})	*b*	2.0−3.7[c]	1.4−2.4[c]

[a] Emission of Ru(bpy)$_3$ could not be observed in our experimental conditions. [b] The transient absorption could not be detected. [c] These values are estimated from the changes of absorbance (ΔA) at 560 nm (deoxy form) and 630 nm (met form).

Table 2. Quantum Yields of Photoactivation of Ru(bpy)$_3$-Mb(**1a**, **1b**, **1c**) at 25 °C, [Na_2EDTA] = 1.0 mM, pH 6.5, 50 mM KH_2PO_4 Buffer

	intermolecular system	Mb(**1a**)	Mb(**1b**)	Mb(**1c**)
Φ_{N_2} ($\times 10^{-4}$)[a]	0.0	0.3	3.4	3.2
Φ_{O_2} ($\times 10^{-4}$)[a]	<0.1	0.3	3.1	2.8

[a] Φ_{N_2} and Φ_{O_2} indicate quantum yield under N_2 atmosphere and aerobic conditions, respectively.

lifetime of Mb(**1b**) (21 ns) was almost identical to that at neutral pH (22 ns). A transient absorption spectrum, however, was not obtained unlike at neutral pH. These results suggest that the back ET was accelerated at basic pH, so we could not isolate transient absorption within our experimental time scale.[16] Scheme 3 and Table 1 summarize the photophysical process and kinetic data of the photoinduced ET of Ru(bpy)$_3$-Mbs based on these laser photolysis studies.

Photoactivation of Ru(bpy)$_3$-Mbs under Aerobic Conditions. Light-driven activation of Ru(bpy)$_3$-Mb was then examined under aerobic conditions. Steady-state photoirradiation quantitatively converted met-Mb to oxy-Mb with six isosbestic points (344, 415, 477, 526, 595, and 670 nm) as shown in Figure 6a. Since dioxygen binding to deoxy-Mb is very rapid, the intermediate deoxy form cannot be spectrophotometrically detected.[17] Oxy-Mb(**1b**) or Mb(**1c**) was slowly autooxidized to the met form with a lifetime of about 10 h, a value comparable to that of native Mb.[18] The spacer effect and pH dependence under aerobic conditions (Figure 6b) were identical to those of photoreduction under anaerobic conditions. The quantum yield (Φ) of the photogeneration of oxy-Mb was similar to that of deoxy-Mb (Table 2).[19] The emission lifetime of *Ru(bpy)$_3$ in Ru(bpy)$_3$-Mb was not influenced by O_2 concentration, unlike the intermolecular system (608 ns under Ar atmosphere, 403 ns under air). Thus, when we turned light on and off under air, the oxy form, an active state of Mb, was completely regulated by visible light (Figure 6c).

Discussion

The steady state and flash photolysis experiments summarized the photoactivation pathway of Ru(bpy)$_3$-Mbs as shown in Scheme 3.[20] The electron transfer from the photoexcited Ru(bpy)$_3$ to heme center (Fe^{3+}) produces the reduced heme (Fe^{2+}) in Mb which can bind dioxygen. But this charge-separated state disappeared to the original state through the back ET without EDTA. In the case of Mb(**1a**), the charge-separated state too rapidly disappeared to react with EDTA, so that the photoactivation efficiency becomes lower than the other Mbs(**1b**, **1c**).

The steady-state photoirradiation experiments revealed a moderate spacer effect as follows. No photoreduction occurred without a connection between Ru(bpy)$_3$ and Mb (the intermolecular control system). The photoreaction of Ru(bpy)$_3$-Mb(**1a**) bearing the shortest spacer was least efficient compared with the other two derivatives (Mb(**1b**) and Mb(**1c**)). The levels of photoreduction efficiency of Mb(**1b**) and Mb(**1c**) were essentially identical. The present spacer effect can be reasonably explained by the results of the laser photolysis. ET from Ru(bpy)$_3$ to heme is not efficiently photoinduced in the intermolecular system. The lifetime of the charge separation state of Mb(**1a**) is too short for observation. The distances between Ru center and iron can be estimated to be 14.3 Å for Mb(**1a**), 21.2 Å for Mb(**1b**), 25.1 Å for Mb(**1c**), if we assume the all trans conformation of the corresponding spacers.[21] The driving force for ET is practically identical in the Ru(bpy)$_3$-Mbs series and it is rather reasonable to suppose that the reorganization energy (λ) of the Marcus equation is almost same in Mb(**1a**),

(16) The OH^--coordinated Fe^{2+}-Mb was not detected using the $Na_2S_2O_4$ reduction system. (a) Wilting, J.; Raap, A.; Braams, R.; De Bruin, S. H.; Rollema, H. S.; Janssen, L. H. M. *J. Biol. Chem.* **1974**, *249*, 6325. (b) Olivas, E.; De Waal, D. J.; Wilkins, R. G. *J. Biol. Chem.* **1977**, *252*, 4038.

(17) Light, W. R.; Rohlfs, R. J.; Palmer, G.; Olson, J. S. *J. Biol. Chem.* **1987**, *262*, 46.

(18) The autoxidation rate constants for oxy-Ru(bpy)$_3$-Mb(**1a**, **1b**, **1c**) were 0.06, 0.04, and 0.06 h^{-1}, respectively. (The rate for native Mb was reported to be 0.08−0.22 h^{-1}.) Brown, W. D.; Mebine, L. B. *J. Biol. Chem.* **1969**, *244*, 6696.

(19) Under aerobic conditions, the photogeneration of oxy-Mb in intermolecular control slightly (less than 10%) occurred, unlike that under anaerobic conditions. This may be attributed to the side reaction with superoxide which generated by ET from *Ru(bpy)$_3^{2+}$ to dioxgen in the intermolecular control system. This side-process does not take place in the intramolecular Ru(bpy)$_3$-Mbs.

(20) Emission intensity of Ru(bpy)$_3$ in steady-state fluorescence and the emission lifetime in laser photolysis do not change upon addition of EDTA (40 mM), suggesting that Ru(bpy)$_3^+$ through the reductive quenching of *Ru(bpy)$_3^{2+}$ by EDTA is not responsible to this reaction pathway.

(21) These values can be estimated by *Chem.3D*.

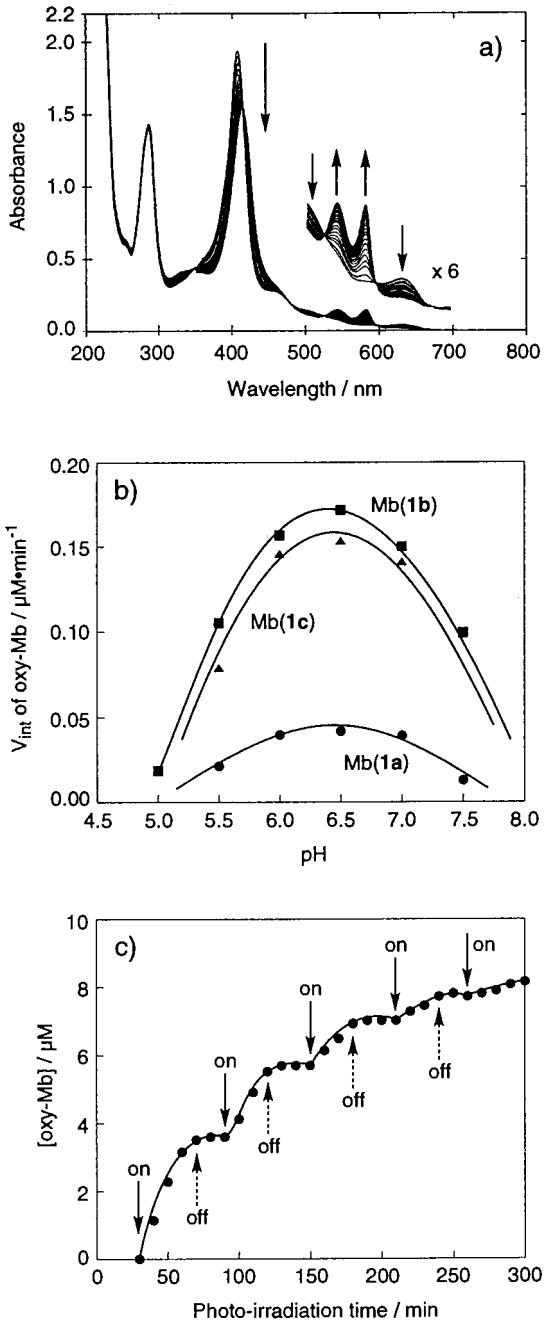

Figure 6. (a) Spectral changes during photogeneration of oxy-Ru(bpy)$_3$-Mb (**1b**) (18.6 μM, Na_2EDTA 10 mM, 50 mM phosphate buffer, pH 6.5, 25 °C) by steady-state photoirradiation under aerobic conditions. (b) The initial rate of the formation of oxy-Ru(bpy)$_3$-Mb depending on pH and the spacer. ●, Mb(**1a**); ■, Mb(**1b**); ▲, Mb(**1c**). (c) Effects of light on Ru(bpy)$_3$-Mb under aerobic conditions. Solid and dashed arrows indicate that visible light (>450 nm, Hg lamp) is switched on or off, respectively. 8.8 μM Ru(bpy)$_3$Mb (**1b**) and 10 mM Na_2EDTA in phosphate buffer (50 mM, pH 6.0) at 25 °C.

Mb(**1b**) and Mb(**1c**). Upon the assumption of β value, the ratio of k_{et} for Mb(**1b**) over k_{et} for Mb(**1c**) can be calculated to be 2.3×10 (for $\beta = 0.8$ Å^{-1}) or 3.3×10 (for $\beta = 0.9$ Å^{-1}).[22] In contrast, actual ET and back ET rates[23] of Mb(**1b**) scarcely differed from those of Mb(**1c**) (the ratio = 1.2), indicating that flexible spacers consisting of oxyethylene units do not rigidly fix the distance between Ru(bpy)$_3$ and the heme center of Mb. However, it is at least clear that both the too short distances (Mb(**1a**), 14.3 Å) and the too long distance (the intermolecular system) are less effective than the moderate distances (Mb(**1b**, **1c**)). Thus, these results suggest that there is an optimum distance for the most efficient photoactivation of Mb.

The bell-shaped rate−pH profile may be ascribed to the pK_a values of EDTA and the coordinated H_2O of the iron(III) center of Mb.[24] At acidic pH, EDTA is predominantly protonated and cannot donate electrons.[25] At basic pH, the axial ligand (H_2O) gradually replaces with a hydroxide anion. The charge separated state of the hydroxide-coordinated Ru(bpy)$_3$-Mb was not detected by our transient absorption measurements, implying that the back ET was too fast for EDTA to reduce the transiently generated Ru^{3+} in the charge separated state.[26] Thus, the activation rate is gradually lessened with increasing pH.

The photoactivation behavior of Ru(bpy)$_3$-Mbs under aerobic conditions (spacer effect, pH dependence and quantum yield) closely resembles those under anaerobic conditions, suggesting that the photoactivation mechanism is essentially same as that under anaerobic conditions as shown in Scheme 3. It is notable that the photogeneration of oxy species is not significantly affected by O_2 although O_2 is a typical quencher of photoexcited Ru(bpy)$_3$. This is mainly due to accelerated intramolecular electron transfer from *Ru(bpy)$_3$ to heme, not to O_2 in Ru-(bpy)$_3$-Mbs.[27]

Conclusion

We demonstrated that chemically modified cofactor-reconstitution can be used to design and semisynthesize photoactive proteins and enzymes. Active-site-directed modification is a unique feature of this method. A wide variety of spacer structures such as peptides, oligonucleotides or noncovalent bonds may be selected to examine mediator properties. Furthermore, a rationally designed photosensitizer−cofactor hybrid should facilitate electrical communication so that the *net* activity of a holoprotein can be controlled by external signals such as visible light. This concept has been expanded to include other hemoproteins or flavoenzymes.[28] In combination with other techniques such as site-directed mutagenesis, chemical modification, peptide semisynthesis, and unnatural amino acid incorporation using suppressor t-RNA, the cofactor-reconstitution technique will be able to create supramolecular proteins with novel biological functions.

(22) The value of β (0.8 ± 0.1) determined previously for electron transfer in Mb by Gray et al. are used in this calculation: Cowan, J. A.; Upmacis, R. K.; Beratan, D. N.; Onuchic, J. N.; Gray, H. B. *Ann. N.Y. Acad. Sci.* **1989**, *550*, 68.

(23) These rate constants are in agreement with the values reported for ET in Mb with high-driving force. Lamgen, R.; Colón, J. L.; Casimiro, D. R.; Karpishin, T. B.; Winkler, J. R.; Gray, H. B. *J. Bioinorg. Chem.* **1996**, *1*, 221.

(24) The pK_a values of the coordinated H_2O to heme iron of Ru(bpy)$_3$-Mb(**1a**, **1b**, **1c**) were spectrophotometrically determinated to be 8.2, 7.9, and 8.4, respectively.

(25) The pK_a values of EDTA are reported to be 2.00, 2.67, 6.16, and 10.26. Pietrzyk, D. J.; Frank, C. W. *Analytical Chemistry*; Academic Press: London, 1974; pp 435−470.

(26) The reduction rate constant of Ru(bpy)$_3^{3+}$ of Mb(**1b**) with EDTA was estimated to be about 10^{10} M^{-1} s^{-1} by laser photolysis: recovery of the bleached Ru(bpy)$_3^{2+}$ was monitored at 450 nm in the absence and the presence of EDTA (pH = 6.0).

(27) As mentioned above, the excited state of Ru(bpy)$_3$ was effectively quenched by O_2 in the intermolecular system but not in the intramolecular Ru(bpy)$_3$-Mb(**1b**).

(28) (a) Riklin, A.; Katz, E.; Willner, I.; Stocker, A.; Bückmann, A. F. *Nature (London)* **1995**, *376*, 672. (b) This approach is recently applied to Cyt b_{562}: Hamachi, I.; Tanaka, S.; Tsukiji, S.; Shinkai, S.; Shimizu, M.; Nagamune, T. *J. Chem. Soc., Chem. Commun.* **1997**, 1735.

Scheme 4

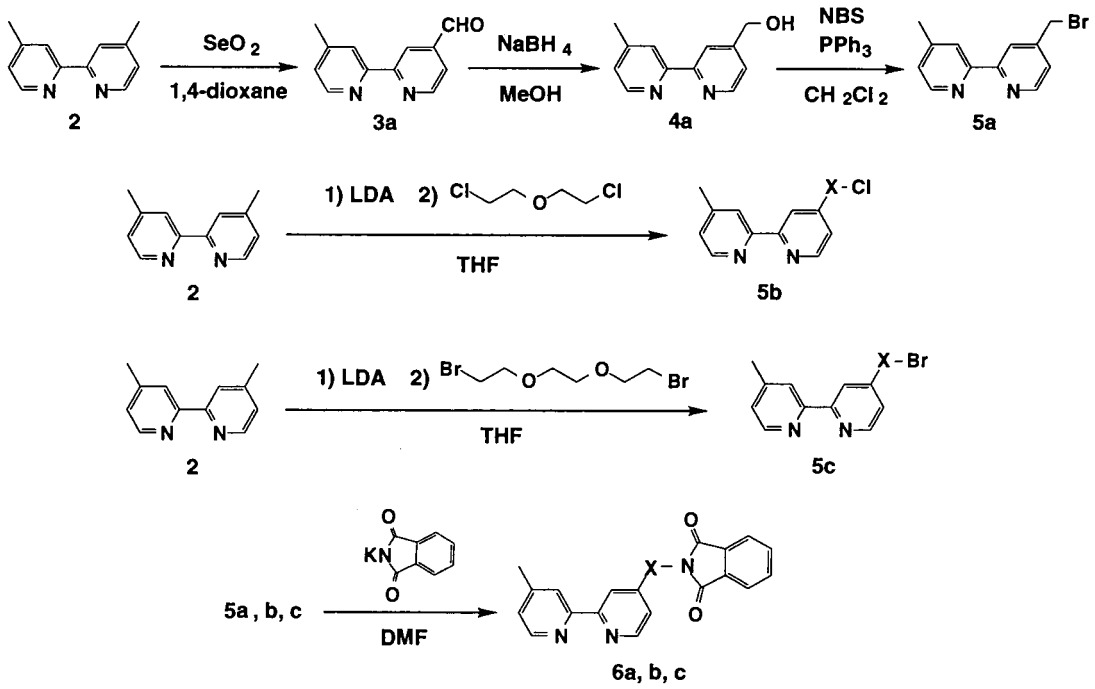

Experimental Section.

Materials. 4,4′-Dimethyl-2,2′-bipyridine,[29] 1,8-dibromo-3,6-dioxaoctane,[30] dichlorobis(2,2′-bipyridine)ruthenium(III) (Ru(III)·(bpy)$_2$·Cl$_2$),[29] and protoporphyrin monoethyl ester (PP-(OEt))[31] were synthesized according to the literature methods. Other chemicals were used without further purification.

Syntheses. (see Scheme 4.) 4-Phthalimidylmethyl-4′-methyl-2,2′-bipyridine 6a.[32] 4-Hydroxymethyl-4′-methyl-2,2′-bipyridine **4a** and **5a** were prepared from 4,4′-dimethyl-2,2′-bipyridine **2** according to the literature method.[33, 34]

5a. Yield 82%, mp = 71.0 °C. ^{1}H NMR (250 MHz, CDCl$_3$, ppm): δ 2.45 (3H, s, −CH$_3$), 4.48 (2H, s, −CH$_2$), 7.15, 7.35, 8.24, 8.41, 8.54, 8.65 (1H each, d, d, s, s, d, d each, pyridine Ar−H).

4-Bromomethyl-4′-methyl-2,2′-bipyridine **5a** (0.54 g, 1.22 mmol) and potassium phthalimide (1.14 g, 6.16 mmol) were stirred in 30 mL of dry DMF (*N*,*N*-dimethylformamide, distilled over NaH) at 40 °C for 1 h under N$_2$ atmosphere. To the mixture was added 100 mL of distilled water, and the mixture was then extracted with dichloromethane (50 mL × 3). The organic layer was collected, dried over Na$_2$SO$_4$, and concentrated. The residue was purified using alumina-column chromatography (eluent: hexane/ethyl acetate = 1/1 v/v). The third fraction was collected and dried in vacuo to yield a white solid **6a** 0.46 g (64%), mp = 66.2 °C. IR (KBr, cm^{-1}): 1710 ($\nu_{C=O}$). ^{1}H NMR (250 MHz, CDCl$_3$, ppm): δ 2.43 (3H, s, −CH$_3$),4.95 (2H, s, −CH$_2$), 7.14, 7.29, 8.19, 8.31, 8.50, 8.59 (1H each, d, d, s, s, d, d each, pyridine, Ar−H), 7.40, 7.88 (2H each, m each, phthalimide Ar−H).

4-(6-Phthalimidyl-4-oxahexyl)-4′-methyl-2,2′-bipyridine 6b.[32,35] Into a solution of 4,4′-dimethyl-2,2′-bipyridine **2** (3.0 g, 16.3 mmol) dissolved in 70 mL of dry THF (distilled over NaH), 2.0 M LDA in THF (lithium diisopropylamide, 10 mL, 19.9 mmol) was added dropwise for 15 min below 0 °C under N$_2$ atmosphere. After addition of bis(2-chloroethyl) ether (19.0 mL, 162.8 mmol) at 0 °C, the mixture was stirred at room temperature under N$_2$ atmosphere overnight. The reaction was quenched by 20 mL of distilled water. After addition 15 mL of saturated NaCl aq, the aqueous layer was extracted with ether (100 mL × 1, 50 mL × 1). The organic layer was dried over Na$_2$SO$_4$ and concentrated. The excess amount of bis(2-chloroethyl) ether was then removed by distillation under reduced pressure (50 °C/0.06 Torr) to give the crude 4-(6-chloro-4-oxahexyl)-4′-methyl-2,2′-bipyridine **5b**. The crude **5b** (2.41 g, 8.29 mmol) and potassium phthalimide (2.72 g, 12.44 mmol) were dissolved in 30 mL of dry DMF and heated at 80 °C for 20 h under N$_2$ atmosphere. After the solution was cooled to room temperature, precipitates were filtered off. The filtrate was concentrated under reduced pressure. Into the residue was added 20 mL of distilled water, and the aqueous layer was extracted with chloroform (20 mL × 3). The combined organic layer was dried over Na$_2$SO$_4$ and evaporated. Purification of the oily residue by column chromatography (neutral alumina, eluent: hexane/ethyl acetate = 1/1 v/v) gave compound **6b** as a white crystalline solid: 1.98 g (59%), mp = 67.2 °C. IR (neat, cm^{-1}): 1710 ($\nu_{C=O}$). ^{1}H NMR (60 MHz, CDCl$_3$, ppm): δ 1.90 (2H, m, -CH$_2$-), 2.43 (3H, s, -CH$_3$), 2.73 (2H, t, Ar-CH$_2$-), 3.68 (6H, m, -CH$_2$-N, -O-CH$_2$-), 7.10, 8.20, 8.51 (2H each, s, d, d, bipyridine Ar-H), 7.78 (4H, d, J = 2.94 Hz, phthalimide Ar-H).

4-(9-Phthalimidyl-4,7-dioxanonyl)-4′-methyl-2,2′-bipyridine 6c.[32,35] Bromo (**5c**) and phthalimide (**6c**) derivatives were prepared according to methods similar to those of **5b** and **6b**, respectively. **5c**. ^{1}H NMR (250 MHz, CDCl$_3$, ppm): δ 2.01 (2H, m, -CH$_2$-), 2.44 (3H, s, -CH$_3$), 2.79 (2H, t, Ar-CH$_2$-), 3.49 (2H each, m, -CH$_2$-Br, 3, -CH$_2$-O-) 3.64 (2H, t, -O-CH$_2$-CH$_2$-O-), 3.82 (2H, m, 8, -O-CH$_2$-), 7.13, 8.23, 8.53 (2H each, m, d, q, pyridine Ar-H. **6c**. Yield 34%. IR (neat, cm^{-1}): 1710 ($\nu_{C=O}$). ^{1}H NMR (CDCl$_3$, 60 MHz, 25 °C, TMS, ppm): δ 2.01 (2H, m, -CH$_2$-), 2.43 (3H, s, -CH$_3$), 2.73 (2H, t, Ar-CH$_2$-), 3.49, 3.54, 3.65, 3.75, 3.91 (2H each, q, q, t, t, m, -O-CH$_2$-), 7.31, 8.23, 8.54 (2H each, d each, t, pyridine, Ar-H), 7.68, 7.81 (2H each, d each, phthalimide, Ar-H).

4-Aminomethyl-4′-methyl-2,2′-bipyridine 7a.[32] The bipyridyl phthalimide **6a** (0.40 g, 1.22 mmol) and hydrazine monohydrate (0.6 mL, 12.22 mmol) were mixed in EtOH (40 mL), and the solution was refluxed for 7 h. After cooling, it was poured into 50 mL of saturated NaCl aq solution. The aqueous solution was basified (pH 12) with 50% NaOH aq, and extracted with CH$_2$Cl$_2$ (50 mL × 3). The combined CH$_2$Cl$_2$ extracts were dried over Na$_2$SO$_4$ and evaporated in vacuo to

(29) Sprintschnik, G.; Sprintschnik, H. W.; Kirsch, P. P.; Whitten, D. G. *J. Am. Chem. Soc.* **1977**, *99*, 4947.
(30) Luttringhaus, A.; Cramer, F.; Prinzbach, H.; Henglein, F. M. *Ann. Chem.* **1958**, *613*, 185.
(31) Regio-isomers were not separated in this study. Tsuchida, E.; Nishide, H.; Sato, Y.; Kaneda, M. *Bull. Chem. Soc. Jpn.* **1982**, *55*, 1890.
(32) Geren, L.; Hahm, S.; Durham, B.; Millett, F. *Biochemistry* **1991**, *30*, 9450.
(33) Imperiali, B.; Prins, T. J.; Fisher, S. L. *J. Org. Chem.* **1993**, *58*, 1613.
(34) Abrena, H. D.; Breikss, A. I.; Collum, D. B. *Inorg. Chem.* **1985**, *24*, 987.
(35) Ciana, L. D.; Hamachi, I.; Meyer, T. J. *J. Org. Chem.* **1989**, *54*, 1731.

give pale yellow oil **7a**. 0.22 g (90%). **7a**. IR (neat, cm^{-1}) 1590 (δN−H). ^{1}H NMR (250 MHz, $CDCl_3$, ppm): δ 1.70 (2H, s, -NH_2), 2.45 (3H, s, -CH_3), 3.99 (2H, s, -CH_2-), 7.14, 7.28, 8.28, 8.34, 8.53, 8.62 (1H each, d, d, s, s, d, d, pyridine Ar-H).

4-(6-Amino-4-oxahexyl)-4′-methyl-2,2′-bipyridine 7b.[32] The amino bipyridyl derivatives **7b** and **7c** were synthesized according to the same method as that of **7a**. **7b**. Yield 93%. IR (neat, cm^{-1}): 3350 (νN−H). ^{1}H NMR (250 MHz, $CDCl_3$, ppm): δ 1.49 (2H, bs, -NH_2), 1.98 (2H, m, -CH_2-), 2.43 (3H, s, -CH_3), 2.83 (4H, m, Ar-CH_2-, -CH_2-N), 3.50 (4H, m, -O-CH_2-), 7.13, 8.24, 8.55 (2H each, q, d, d, bipyridine Ar-H).

4-(9-Amino-4,7-dioxanonyl)-4′-methyl-2,2′-bipyridine 7c.[32] **7c**. Yield 90%. IR (neat, cm^{-1}) 1590 (δN−H), 3350 (νN−H). ^{1}H NMR ($CDCl_3$, 250 MHz, 25 °C, TMS, ppm): δ 1.90 (2H, bs, -NH_2), 2.03 (2H, m, -CH_2-), 2.43 (3H, s, -CH_3), 2.80 (2H, t, Ar-CH_2-), 2.88 (2H, s, -CH_2-N), 3.53, 3.63 (4H each, q, t, -CH_2-O-), 7.15, 8.23, 8.56 (2H each, t, t, t, pyridine, Ar-H).

3,8,12,18-Tetramethyl-2,7-divinyl-17-[2-(ethoxycarbonyl)-ethyl]-13-[2-(*N*-{2-[3-(4′-methyl-2,2′-bipyridine-4-yl)propoxyl]-ethyl}-carbamoyl)ethyl]porphine 8a.[36] To a dry THF solution containing the amino bipyridyl derivative **7a** (0.22 g, 1.10 mmol) and PP−(OEt), (0.30 g, 0.51 mmol), diethylcyanophosphate (DEPC, 1.00 g, 6.13 mmol) was added with ice-cooling. After the mixture was stirred for 10 h at 0 °C under N_2 atmosphere, the solution was neutralized to pH = 7 with triethylamine. After THF was evaporated off, the residue dissolved in 100 mL of $CHCl_3$ was washed with $NaHCO_3$ aq (50 mL × 2). The organic layer was dried over Na_2SO_4. Evaporation gave a crude product, which was purified by reprecipitation ($CHCl_3$/MeOH) and washing with EtOH. Dark solid **8a** was obtained (0.25 g, 64%), mp = 214.0 °C. IR (KBr, cm^{-1}): 1720 ($\nu_{C=O}$), 1640 ($\nu_{C=O}$). ^{1}H NMR (250 MHz, $CDCl_3$, ppm): δ −4.07 (2H, bs, pyrrole, NH) 0.66 (3H, t, -CH_2), 2.31 (3H, s, Ar-CH_3), 3.13 (4H, m, 13^2, 17^2, -CH_2-), 3.48, 3.70 (14H, m each, 2, 7, 12, 18, -CH_3, -O-CH_2-), 4.38−4.71 (6H, m each, 13^1, 17^1, -CH_2-, Ar-CH_2-), 6.12, 6.18, 6.29, 6.36 (4H, s each, =CH_2), 6.61, 6.85, 7.87, 7.96 (4H, d, d, s, s each, pyridine, Ar-3, 3′, 5, 5′H), 6.97 (1H, d, -NH), 8.05−8.26 (4H, m, -CH=, pyridine, Ar-6, 6′H), 9.86−10.05 (4H, m, *meso*-H). Found: C, 74.30; H, 6.37; N, 12.36. Calcd for $C_{48}H_{49}N_7O_3$: C, 74.66; H, 6.40; N, 12.70.

3,8,12,18-Tetramethyl-2,7-divinyl-17-[2-(ethoxycarbonyl)ethyl]-13-(2-{*N*-[6-(4′-methyl-2,2′-bipyridine-4-yl)-4-oxahexyl]carbamoyl}-ethyl)porphine 8b.[36] **8b** and **8c** were synthesized according to the same method as that of **8a**. Yield 60%, mp = 187.7 °C. IR (KBr, cm^{-1}): 1735 ($\nu_{C=O}$), 1655 ($\nu_{C=O}$), 1550 (δNH). ^{1}H NMR (250 MHz, $CDCl_3$, ppm): δ −4.15 (2H, bs, pyrrole NH) 0.35 (2H, m, Ar-CH_2-), 0.98 (3H, t, -CH_3), 1.73 (2H, m, -CH_2-), 2.26 (3H, s, Ar-CH_3), 2.63 (2H, t, N-CH_2-), 3.16 (8H, m, 13^2, 17^2, -CH_2- and -CH_2-O-CH_2-), 3.54 (12H, m, each, 2, 7, 12, 18, -CH_3), 4.29 (4H, m, each, 13^1, 17^1, -CH_2-), 5.89, 7.39 (1H each, d each, pyridine Ar-3, 3′H) 6.14, 6.31 (2H each, dd each, =CH_2), 6.75 (1H, d, -NH), 8.09 (6H, m, -CH= and pyridine Ar-5, 5′, 6, 6′H), 9.61−10.00 (4H, s, *meso*-H). Found: C, 73.41; H, 6.81; N, 11.51. Calcd for $C_{52}H_{57}N_7O_4$·0.5H_2O: C, 73.02; H, 6.87; N, 11.50.

3,8,12,18-Tetramethyl-2,7-divinyl-17-[2-(ethoxycarbonyl)-ethyl]-13-(2-{*N*-[9-(4′-methyl-2,2′-bipyridine-4-yl)-4,7-dioxanonyl]-carbamoyl}ethyl)porphine 8c.[36] Yield 61%, mp = 194.0 °C. IR (KBr, cm^{-1}): 1730 ($\nu_{C=O}$), 1660 ($\nu_{C=O}$). ^{1}H NMR (250 MHz, $CDCl_3$, ppm): δ −3.91 (2H, bs, pyrrole NH), 1.01 (2H, m, -CH_3), 2.10 (2H, m, -CH_2-), 2.25 (3H, s, Ar-CH_3), 2.77 (2H, t, Ar-CH_2-), 3.15 (4H, m, -CH_2-), 3.25 (2H, m, N-CH_2-), 3.56, 3.74 (4H each, d, d, -OCH_2-), 3.68 (12H, m each, 2, 7, 12, 18, -CH_3), 4.01 (2H, q, -(CO)-O-CH_2-), 4.36 (4H, m each, 13^1, 17^1, -CH_2-), 6.15−6.38 (5H, dd, dd, t each, 3, 8, =CH_2 and Ar-5H), 6.67, 6.80 (1H each, d, d, Ar-3, 3′H), 7.90, 8.06 (1H each, d, d, Ar-6, 6′H), 8.19−8.35 (4H, s, d, t each, -NH and pyridine Ar-5′H and 3, 8, -CH=), 9.95−10.13 (4H, s each, *meso*-H).

{**4-[3-(2-{2-[3,8,12,18-Tetramethyl-2,7-divinyl-17-(2-carboxyethyl)-porphine-13-yl]ethylcarbonylamino}ethoxy)propyl]-4′-methyl-2,2′-bipyridine}[bis(2,2′-bipyridine)]ruthenium(II)·$(ClO_4)_2$ 9a.**[29] **8a** (0.25 g, 0.32 mmol) and Ru(III)·$(bpy)_2$·Cl_2 (0.21 g, 0.41 mmol) were dissolved in 50 mL of dry EtOH (distilled over CaO) and refluxed for 4 h under N_2 atmosphere. After cooling, EtOH was evaporated and the residue was dried under reduced pressure. The residue was dissolved in 20 mL of aqueous EtOH (EtOH/distilled water = 1/1), and the insoluble impurities were removed by filtration. To the filtrate was added 0.1 N-NaOH (6.5 mL, 2.0 eq) and stirred for 12 h at room temperature. The reaction mixture was concentrated and purified with gel-column chromatography (Toyo-pearl HW-50F, eluent MeOH). The first fraction was collected, dried under reduced pressure, and then dissolved in a small amount of distilled water. After removal of the insoluble impurities, the saturated $NaClO_4$ aqueous solution was added to the filtrate. The reddish purple precipitate was collected by filtration, sufficiently washed with distilled water, and dried over reduced pressure to obtain Ru complex **9a**. Yield 0.26 g (58%), mp > 300 °C. IR (KBr, cm^{-1}) 1390, 1550 ($\nu_{C=O}$). ^{1}H NMR (250 MHz, DMSO-d_6, ppm): δ −3.90 (2H, bs, pyrrole, NH) 0.66 (3H, t, -CH_3), 2.78 (3H, s, Ar-CH_2), 3.63, 3.74 (12H, m each, 2, 7, 12, 18, -CH_3), 4.20, 4.39 (4H, m each, 132, 172,-CH_2-), 4.72 (2H, d, Ar-CH_2-), 6.24, 6.44 (4H, d, dd each, =CH_2), 7.30, 7.50, 7.82, 8.17, 8.84, 9.40, 9.65 (22H, d each, m, m, m, m, s, s, pyridine, Ar-H), 8.52 (2H, d, -CH=), 10.30−10.22 (4H, m, *meso*-H). UV−vis spectrum (MeOH, nm): 397 (Soret band), 630 (Q band). Found: C, 56.87; H, 4.92; N, 11.11. Calcd for $C_{66}H_{60}N_{11}O_{11}Cl_3NaRu$·$H_2O$: C, 56.75; H, 4.47; N, 11.04. UV−vis spectrum (MeOH, nm): 403 (Soret band), 503, 538, 573, 630 (each Q band).

[4-(6-{2-[3,8,12,18-Tetramethyl-2,7-divinyl-17-(2-carboxyethyl)-porphine-13-yl]ethylcarbonylamino}-4-oxahexyl)-4′-methyl-2,2′-bipyridine][bis(2,2′-bipyridine)]ruthenium(II)·$(ClO_4)_2$ 9b.[29] Yield 79%, mp > 300 °C. IR (KBr, cm^{-1}): 1610 ($\nu_{C=O}$). ^{1}H NMR (250 MHz, $CDCl_3$, ppm): δ −4.10 (2H, bs, pyrrole NH) 1.21 (2H, m, Ar-CH_2-), 1.62 (2H, m, -CH_2-), 2.26 (3H, t, -CH_3), 2.81 (2H, t, N-CH_2-), 2.90, 3.17 (12H, m each, 2, 7, 12, 18, -CH_3), 3.66 (8H, m, 13^2, 17^2, -CH_2- and -CH_2-O-CH_2-), 4.22 (4H, m, each 13^1, 17^1, -CH_2-), 5.99, 6.43 (2H each, dd each, −CH=) 7.23, 7.46, 7.67, 8.04, 8.66, 8.74 (22H each, t, t, t, m, m, m, bipyridine Ar-H), 8.44 (2H, m, -CH=), 9.70 (1H, bs, -NH), 10.18−10.5 (4H, s each, *meso*-H). UV−vis spectrum (MeOH, nm): 408 (Soret band), 503, 538, 574, 630 (each Q band).

[4-(9-{2-[3,8,12,18-Tetramethyl-2,7-divinyl-17-(2-carboxyethyl)-porphine-13-yl]ethylcarbonylamino}-4,7-dioxanonyl)-4′-methyl-2,2′-bipyridine][bis(2,2′-bipyridine)]ruthenium(II)·(ClO_4)·Cl 9c.[29] Yield 48%, mp > 220 °C, decomp. IR (KBr, cm^{-1}): 1390 ($\nu_{C=O}$), 1550 ($\nu_{C=O}$). ^{1}H NMR (250 MHz, DMSO-d_6, ppm): δ 1.80 (2H, m, -CH_2-), 2.35 (3H, t, Ar-CH_3), 2.72 (2H, m, Ar-CH_2-), 2.99 (2H, m, N-CH_2-), 3.21 (12H, m, 2, 7, 12, 18, -CH_3), 3.34 (4H, m, 13^2, 17^2, -CH_2-), 3.47, 3.60 (4H each, m, -O-CH_2-), 4.17, 4.26 (2H each, bs, bs, 13^1, 17^1, -CH_2-), 6.16, 6.36 (2H each, dd each, =CH_2) 7.27, 7.36, 7.50, 7.69, 8.08, 8.75 (22H, d, d, m, q, m, m each, pyridine Ar-H), 8.34 (2H, m, -CH=), 10.45 (1H, bs, -NH), 9.95−10.61 (4H, s each, *meso*-H). UV−vis spectrum (methanol, nm): 408 (Soret band), 503, 538, 574, 630 (each Q band).

Iron(III) Complex 1a from 9a.[37] The free base **9a** (70 mg, 0.03 mmol) and $FeCl_2$·$4H_2O$ (64 mg, 0.51 mmol) dissolved in 10 mL of dry DMF were heated at 65 °C with stirring for 4 h under N_2 atmosphere. DMF was evaporated off and acidic brine (pH 3, 10 mL) was added to the residual solid. The suspension was vigorously stirred for 30 min at room temperature, centrifuged (10 000 rpm), and then the insoluble solid was sufficiently washed with distilled water. After drying over, the crude precipitation was purified with gel-column chromatography (Sephadex LH-20, eluent MeCN) to yield a black solid **1a**. Yield 24 mg (33%), mp > 300 °C. IR (KBr, cm^{-1}): 1390, 1550 ($\nu_{C=O}$). Found: C, 54.46; H, 4.18; N, 10.17. Calcd for $C_{66}H_{59}N_{11}O_{11}Cl_3FeRu$·$H_2O$: C, 54.16; H, 4.20; N, 10.52. UV−vis spectrum (MeOH, nm), 404 (Soret band), 630 (Q band).

Iron(III) Complex 1b from the Ruthenium(II) Complex 9b.[37] Yield 79%, mp > 300 °C. IR (KBr, cm^{-1}): 1710 ($\nu_{C=O}$). Found: C, 51.78; H, 4.53; N, 9.28. Calcd for $C_{70}H_{67}N_{11}O_{12}Cl_3FeRu$·$5H_2O$: C, 52.27; H, 4.82; N, 9.58. UV−vis spectrum (MeOH, nm): 397 (Soret band), 630 (Q band).

Iron(III) Complex 1c from the Ruthenium(II) Complex 9c.[37] Yield 17%, mp > 300 °C. IR (KBr, cm^{-1}) 1710 ($\nu_{C=O}$). Found: C,

(36) Yamada, S.; Kasai, Y.; Shioiri, T. *Tetrahedron Lett.* **1873**, *18*, 1595.

(37) Murakami, H.; Nagasaki, T.; Hamachi, I.; Shinkai, S. *Tetrahedron Lett.* **1993**, *14*, 6273.

55.75; H, 4.93; N, 9.88. Calcd for $C_{72}H_{71}N_{11}O_9Cl_3FeRu \cdot 3H_2O$: C, 55.73; H, 5.00; N, 9.92. UV−vis spectrum (MeOH, nm): 400 (Soret band), 630 (Q band).

Reconstitution of apo-Mb with Ru(bpy)$_3$-Hemin (1a−c). The apo-Myoglobin was prepared from horse heart myoglobin (Sigma) by Teale's acid/butanone procedure.[8a] Reconstitution of Ru(bpy)$_3$-hemin with apo-Mb was conducted according to the modified method of Yonetani et al.[8b] To apo-Mb solution (50 mM phosphate buffer, pH 7.0) was added dropwise 1.2 equiv of Ru(bpy)$_3$-hemin dissolved in pyridine (**1a** and **1b** in pyridine, **1c** in pyridine: phosphate buffer (50 mM, pH 6.0)). The mixture was moderately stirred for 5 min and dialyzed against 50 mM KH_2PO_4 buffer (pH 7.0, several times), then against phosphate buffer (pH 6.5), and finally against phosphate buffer (pH 6.0). After centrifuge at 4 °C for 10 min, the clear supernatant was purified with Sephadex G-25 (equilibrated with a 50 mM phosphate buffer at pH 6.0) at 4 °C. The concentrations of Ru(bpy)$_3$-Mb (**1a**−**c**) were determined spectrophotometrically ($\epsilon_{408\ nm}$ = 160 000 (**1a**), 117 000 (**1b**), and 91 000 (**1c**) determined by the pyridine−hemochrome method[36]). Yield: Mb(**1a**), 70%; Mb(**1b**), 72%; Mb(**1c**), 22%.

Photoirradiation to Reconstituted Ru(bpy)$_3$-Mbs (1a−c). To Ru(bpy)$_3$-Mb (**1a**−**c**) dissolved in phosphate buffer (50 mM, pH 5.5−8.0) was added ethylenediaminetetraacetic acid disodium salt (Na_2-EDTA). pH was adjusted with NaOH aq to the corresponding value. In the case of anaerobic photoreduction, the solutions were gently purged with N_2 gas and then carefully degassed by freeze−pump−thaw cycles. Photoirradiation to the solutions was carried out with a 400-W high-pressure Hg lump equipped with an optical filter (λ > 450 nm, Toshiba Y-45 glass filter) at 25 °C. Absorption spectral changes were monitored with UV−vis spectroscopy (Shimadzu UV-160 or Hitachi U-3300). Initial rates of the formation of deoxy- or oxy-Mb were calculated from the initial linear portion of the absorbance at 580 or 555 nm against time.

Quantum Yields of the Photoactivation of Ru(bpy)$_3$-Mb (1a−c). Quantum yields of the photoactivation for Ru(bpy)$_3$-Mb (**1a**−**c**) were determined according to the slightly modified literature procedure.[39]

Determination of Redox Potentials Ru(bpy)$_3$-Mbs (1a−c). The oxidation−reduction potentials of Ru(bpy)$_3$-Mbs were determined with the slightly modified procedure reported previously.[10]

Laser Photolysis Experiments. The sample solutions (3 mL) degassed with five freeze−pump−thaw cycles were subjected to pulsed-laser photolysis at 20 °C, using a third harmonic light (355 nm, fwhm = 5 ns) from a Q-switched Nd:YAG laser (Quanta-Ray DCR-11) for excitation. A right-angle optical system was employed for the excitation-analysis setup. Probe lights were detected by a photomultiplier tube (Hamaphoto R446) or a photodiode array (Princeton IRY-1024G/RB, gate width = 4 ns).

Acknowledgment. The authors are grateful to Dr. Hitoshi Ishida for suggestions regarding this collaboration. We thank Professor Keiichi Tsukahara for fruitful discussions. We also thank Mr. Hideki Horiuchi for construction of custom-designed UV−visible cells. S. Tanaka is a fellow of the Japan Society for the Promotion of Science for Japanese Junior Scientists.

IC971507M

(38) Miyashito, N.; Yoshikoshi, A.; Greico, P. A. *J. Org. Chem.* **1977**, *42*, 3772.
(39) Hatchard, C. G.; Parker, C. A. *Proc. R. Soc. London, Ser. A* **1956**, *235*, 518.